Origins of Electronic Band Gap Reduction in Cr/N Codoped TiO_2

C. Parks Cheney,[1] P. Vilmercati,[1] E. W. Martin,[1] M. Chiodi,[2] L. Gavioli,[2] M. Regmi,[3] G. Eres,[3] T. A. Callcott,[1] H. H. Weitering,[1,3,*] and N. Mannella[1,†]

[1]*Department of Physics and Astronomy, The University of Tennessee, Knoxville, Tennessee 37996, USA*
[2]*Dipartimento di Matematica e Fisica and Interdisciplinary Laboratories for Advanced Materials Physics, Università Cattolica del Sacro Cuore di Brescia, Via Musei 41, Brescia 25121, Italy*
[3]*Materials Science and Technology Division, Oak Ridge National Laboratory, Oak Ridge, Tennessee 37831, USA*

(Received 10 July 2013; published 23 January 2014)

Recent studies indicated that noncompensated cation-anion codoping of wide-band-gap oxide semiconductors such as anatase TiO_2 significantly reduces the optical band gap and thus strongly enhances the absorption of visible light [W. Zhu *et al.*, Phys. Rev. Lett. **103**, 226401 (2009)]. We used soft x-ray spectroscopy to fully determine the location and nature of the impurity levels responsible for the extraordinarily large (∼1 **eV**) band gap reduction of noncompensated codoped rutile $\mathbf{TiO_2}$. It is shown that **Cr/N** codoping strongly enhances the substitutional N content, compared to single element doping. The band gap reduction is due to the formation of Cr $3\boldsymbol{d}^3$ levels in the lower half of the gap while the conduction band minimum is comprised of localized Cr $3\boldsymbol{d}$ and delocalized N $2\boldsymbol{p}$ states. Band gap reduction and carrier delocalization are critical elements for efficient light-to-current conversion in oxide semiconductors. These findings thus raise the prospect of using codoped oxide semiconductors with specifically engineered electronic properties in a variety of photovoltaic and photocatalytic applications.

DOI: 10.1103/PhysRevLett.112.036404 PACS numbers: 71.20.Nr, 61.72.S-, 78.70.Dm, 79.60.-i

In developing novel materials with tunable optical, electronic, and chemical functionality, proper introduction of a foreign species into a host material via chemical substitution or "doping" has been one of the most powerful methods for altering or tuning the basic electronic band structure of an intrinsic semiconductor [1]. While doped Si, and to a lesser extent III-V semiconductors, still are the most commonly used semiconductors, there has always been a need for developing alternative semiconductor materials with novel or complementary functionality at reduced cost. For instance, binary metal-oxide semiconductors such as SnO_2, In_2O_3, ZnO, Cu_2O, and TiO_2 have been vigorously pursued in a variety of semiconductor applications ranging from optically transparent conductors [2], photovoltaics [3], photocatalysis [4], and spintronics [5].

An overview of the results reported in the literature exposes a fundamental fact, namely, the *extreme difficulty* in doping binary oxide semiconductors in a controlled manner [6–9]. Specifically, while it may be possible to dope an oxide semiconductor as *n*type, it would then be almost impossible to incorporate *p*-type dopants, or vice versa [8]. In particular, oxygen substitution is difficult to accomplish. Oxide dopants often have very limited solubility and it is often unclear whether they are substitutional, interstitial, incorporated in grain boundaries, or if they form dopant complexes such as dopant pairs or complexes that involve cation interstitials and/or anion vacancies [10]. A conceptual breakthrough is clearly needed to identify dopants that are thermodynamically stable at substitutional lattice locations in oxide lattices and produce donor or acceptor levels at desirable locations in the host band gap. The case of titanium dioxide (TiO_2) underscores these difficulties. Considered the most promising photocatalyst for solar energy utilization, its intrinsic wide band gap (≈3 eV) results in a photocatalysis efficiency well below the 10% target for commercial and industrial applications. Band gap narrowing in TiO_2 has been recognized as the main avenue for enhancing its performance in photoelectrochemical energy conversion, but numerous attempts based on conventional doping schemes have proven to be rather ineffective [11]. Recently, density functional theory (DFT + U) calculations indicated that the introduction of a noncompensated dopant *pair*, i.e., a double donor (e.g., Cr) combined with a single acceptor (e.g., N) or vice versa (e.g., V, C), into *anatase* TiO_2 is an effective method for enhancing the thermodynamic solubility of the dopants and for the formation of wide impurity bands that would effectively shrink the optical band gap of TiO_2 toward the visible range. [12] The latter has indeed been observed in optical absorption experiments on sol-gel powder samples [12].

In this Letter, we elucidate the lattice location of the dopants and the orbital nature of the dopant-induced electronic states in Cr-N codoped TiO_2. We show that noncompensated codoping also enhances the solid solubility of the N dopant in the oxygen sublattice of *epitaxial rutile* TiO_2 and reduces its band gap by about 1 eV. Notably, the origin of the band gap reduction is different from the one suggested theoretically for anatase [12]. Whereas DFT + U calculations for anatase attributed the band gap narrowing to the formation of an *n*-type impurity band in the upper part of the gap [12], we find that the band gap

narrowing in rutile is completely accounted for by the formation of a Cr-derived impurity band in the lower part of the band gap [13]. In addition, the data reveal the existence of a delocalized N-derived impurity band that is degenerate with the conduction band (CB) minimum. Such delocalization of the photoinduced charge carriers, which is notoriously difficult to achieve in oxides by conventional doping, is at the heart of the light-to-current conversion processes in photovoltaic and photocatalytic applications. By elucidating the microscopic mechanisms underpinning effective doping of oxide semiconductors, our data indicate that noncompensated codoping raises the prospect of using oxide semiconductors with specifically engineered electronic properties in a variety of photovoltaic and photocatalytic applications.

Doped TiO_2 thin films were epitaxially grown on single-crystal $LaAlO_3$ substrates with pulsed laser deposition (PLD; see the Supplemental Material [14]). PLD synthesis is capable of producing novel phases that are inaccessible by equilibrium synthesis methods, which facilitates dopant incorporation at levels well beyond the solid solubility limit. Interestingly, while in single N or Cr doped TiO_2 the anatase structure is usually formed, [15] PLD synthesis of codoped samples grown at temperatures below ≈600 °C is found to stabilize the rutile phase (see the Supplemental Material [14]). The following data have been taken at room temperature from codoped rutile samples grown at 350 °C. Additional experimental details and methodologies are described in the Supplemental Material [14].

Core level and VB photoemission (PES) measurements address two fundamental aspects of codoping, i.e., N dopant solubility and band gap reduction. The PES spectra of the VB shown in Fig. 1(a) provide direct evidence for the formation of an impurity band in the lower part of the gap and a ∼1 eV reduction of the portion of the band gap below the Fermi level (E_F) as compared to pure TiO_2 [16]. Figure 1(b) shows PES spectra of the N 1s core level in N-doped and Cr/N codoped samples grown under identical conditions. The component at lower BE (∼396 eV) is attributed to substitutional N, [17] largely predominant in the codoped sample. Cr/N codoping appears to be much more effective in incorporating substitutional N into the rutile phase than conventional doping under similar conditions.

Incorporation of Cr into substitutional sites is equally important, but easier to achieve. The Cr 2p core level spectrum is very similar to that of Cr_2O_3 [18] while the Cr 3s spectrum exhibits an exchange splitting of 3.9 eV [19] (see the Supplemental Material [14]). These observations indicate that Cr is present as Cr^{3+}, similar to the substitutional Cr dopants inside Cr-doped TiO_2 [20]. The Cr $3d^3$ configuration in Cr-N codoped TiO_2 suggests the presence of two holes on the O and/or N ligands (see the Supplemental Material [14]). These two holes could in principle be filled via the creation and ionization of a single O vacancy. Quantitative PES analysis indicates a Cr:N content of

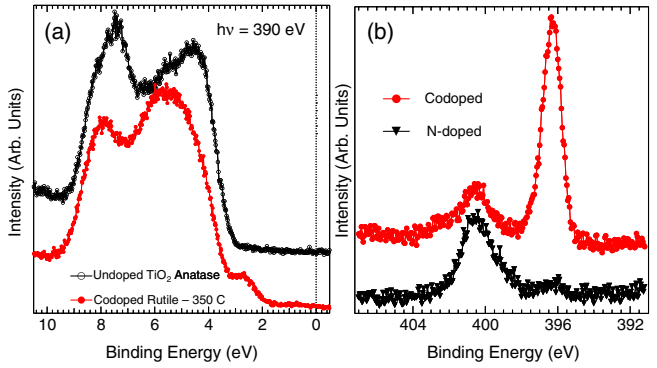

FIG. 1 (color online). (a) Comparison of VB PES spectra excited with photon energy $h\nu = 390$ eV of a Cr/N codoped rutile sample grown at 350 °C and a pure TiO_2 sample, showing the formation of an impurity band in the codoped sample. (b) N 1s core level PES spectrum excited with monochromatic photon energy $h\nu = 1486.6$ eV in N-only doped and Cr/N codoped samples grown at 350 °C. Samples have been grown under similar conditions. The N 1s spectrum consists of two components: the one at lower binding energy (BE) is routinely ascribed to substitutional N, while the components at higher BE are associated to nonsubstitutional forms of N.

about $0.06/0.03 = 2$, so it is likely that oxygen vacancies are present to compensate the excess Cr dopants [21], which would explain why the E_F is pinned at the CB minimum (cf. Fig. 2) [8]. There is no evidence in PES for the existence of a reduced Ti^{3+} ($3d^1$) species or $3d^1$ exciton trap states, as is often seen in N-doped rutile TiO_2 or pure TiO_2 with oxygen vacancies [17] (see the Supplemental Material [14]).

To determine the origin of the gap states responsible for the ∼1 eV band gap reduction in the Cr/N codoped rutile samples, we used a combination of x-ray emission spectroscopy (XES), x-ray absorption spectroscopy (XAS), and resonant PES experiments. The XES/XAS spectra were excited following electron emission from the Ti 2p, O 1s, N 1s, and Cr 2p core levels. Considering the dipole selection rules and the major contribution expected from some transitions, the XES (XAS) spectra can be associated with the occupied (unoccupied) Ti 3d, O 2p, N 2p, and Cr 3d levels. The spectra are shown in Fig. 2 after being aligned to a common energy scale obtained by subtracting the BE of the excited core levels from the photon energies and correcting for the core-hole potentials (see the Supplemental Material [14]) [22]. With this procedure, we fully determined the occupied and unoccupied density of states (DOS) in the VB and CB with elemental sensitivity or "partial DOS."

Figure 2 shows that the E_F is pinned near the CB minimum. Notably, the reduction of the band gap mainly originates from the filling of impurity states at the top of the VB, consistent with the PES data shown in Fig. 1(a). This differs from the DFT predictions for anatase, according to which the reduction of the band gap occurs primarily

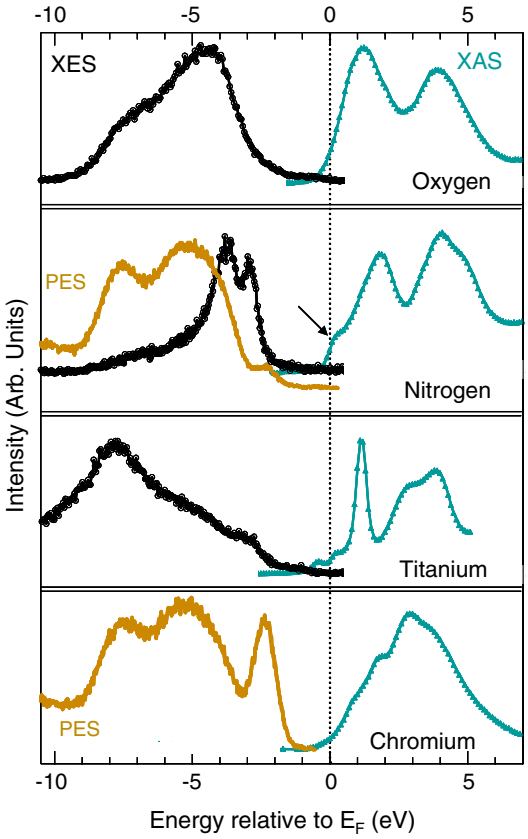

FIG. 2 (color online). O K_α, N K_α Cr L_α, and Ti L_α XAS and XES spectra after correction for the core hole potentials. Also shown are the VB PES spectra measured at resonance on the N K and Cr L edge. The XES and XAS spectra are representative of the projected (i.e., element sensitive) occupied and unoccupied density of states, respectively, modulated by the matrix elements of the transition involved. The relative magnitude of the states relative to different elements are thus not to scale. The XES and XAS spectra are aligned to a common energy scale with the PES spectrum, referenced to the Fermi level, by subtracting the core level binding energies from the energies of the O K_α, N K_α, Cr L_α, and Ti L_α XAS and XES spectra, thus enabling the decomposition of the VB in the N $2p$, O $2p$, Cr $3d$, and Ti $3d$ partial density of states components. The arrow in the nitrogen panel indicates the prepeak structure (see text).

due to the presence of additional unoccupied states appearing at ≈ 1 eV below the CB minimum [13].

The N K_α XAS spectrum consists of two main structures separated by $\approx 2.5-3.0$ eV, which correspond to unoccupied N $2p$ states covalently mixed with the Ti/Cr t_{2g} and e_g manifolds, as is the case for the N K-edge spectra in CrN and TiN, and O K-edge spectra in TiO_2 (see the Supplemental Material [14]) [23]. Importantly, the N near-edge XAS spectrum exhibits a prepeak, i.e., a structure on the low energy side of the spectrum in the proximity of E_F, which has not been observed in the N K-edge XAS spectra in TiN and CrN compounds [24]. The pre-peak structure is indicative of the presence of additional holes in the N $2p$ manifold of the CB. This is fully consistent with the earlier conclusion that the ligands do not have a full $2p$ shell. It also implies that oxygen vacancies, if present, do not fully compensate the $2p$ holes.

The excitation energies for the XES spectra in Fig. 2 were chosen to be $7-8$ eV above threshold in order to provide the best possible representation of the occupied partial DOS [25] (see the Supplemental Material [14]). In this modality of spectra acquisition, the core-hole lifetime produces a long high-energy Lorentzian tail in the XES spectra, making it very hard to accurately perform linear extrapolation of the VB maximum and accurately determine the portion of the band gap below E_F. However, the Lorentzian tail is suppressed close to the threshold excitation energy so that XES spectra can still be exploited for quantitative band gap determination. Figure 3 shows a series of XES spectra excited with photon energies tuned across the Cr L absorption edge (i.e., at the Cr L threshold). This modality of spectra acquisition (i.e., under resonant excitation conditions) is commonly referred to as resonant inelastic x-ray scattering (RIXS). In this case, the photon-in–photon-out process can be viewed as the x-ray analogue of a Raman scattering event, in which the energy difference between the incident and the emitted photon represents an energy loss that corresponds to an excitation on the same atomic site. The spectra shown in Fig. 3 exhibit a constant ≈ 2 eV energy loss which

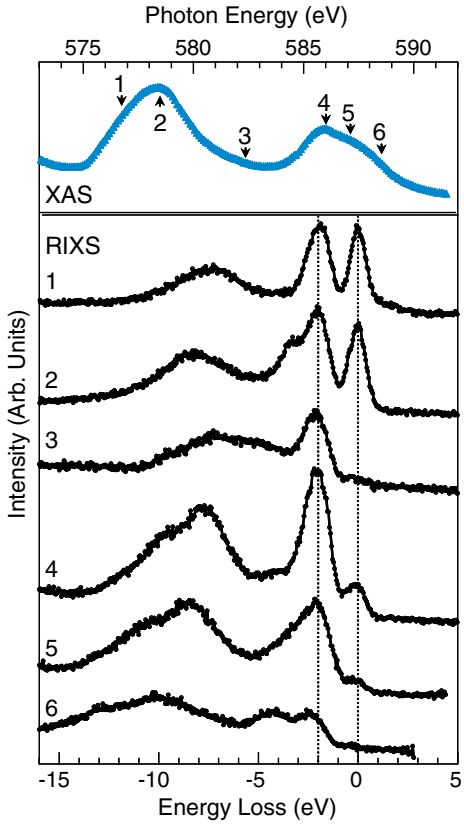

FIG. 3 (color online). Cr RIXS spectra excited with photon energies chosen on the Cr L edge plotted on an energy loss scale with the peak at zero energy denoting the elastic peak. The peak at ≈ 2 eV to the left of the elastic peak is indicative of an energy loss corresponding to Cr d-d transitions across the gap.

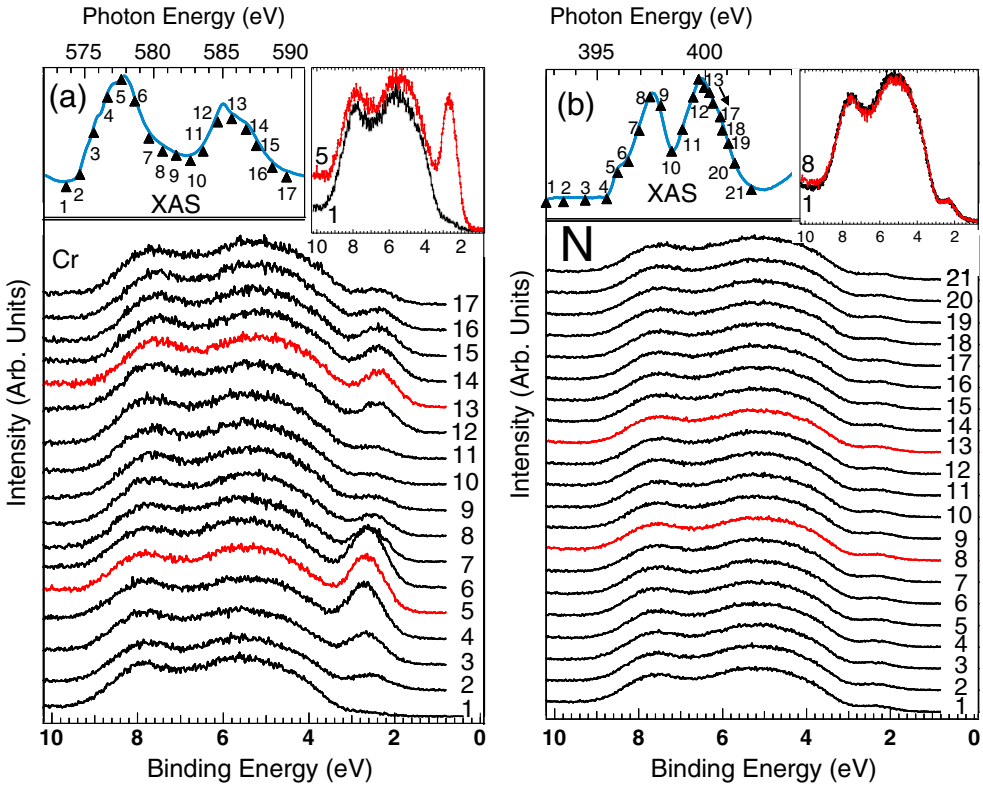

FIG. 4 (color online). ResPES spectra excited with incident photon energy tuned across the (a) Cr L and (b) N K absorption edge. The trace at the top left of both panels is the XAS spectrum, with the points denoting the excitation photon energies. The top right insets show the difference of the spectra on and off resonance.

can be unambiguously identified as the energy of the Cr d-d interband transition across the gap.

PES spectra of the VB are elemental sensitive when the measurements are performed according to a scheme known as resonant PES (ResPES) [26–28]. In a ResPES measurement, the incident photon energy is tuned across the absorption edge of a deeper core level of an atom. The portion of the VB spectrum associated with the resonating energy level(s) is enhanced and thus can be extracted from the total VB structure. This can be observed in VB spectra excited with photon energies tuned across the Cr L edge [cf. Fig. 4(a)]. The peak with BE of ≈ 2.5 eV are states belonging to the Cr $3d$ manifold. A different behavior occurs when VB spectra are measured with photon energies tuned across the N K edge [Fig. 4(b)]. In this case, no enhancement of any part of the VB spectrum could be detected beyond the noise level, a puzzling observation given the fact that the occupied N states extend to the top of the VB, up to ≈ 2 eV below E_F (cf. Fig. 2). The details of the ResPES process provide a rationale for this behavior. In a ResPES experiment, one electron is promoted from the core level to an unoccupied state above E_F in the CB, leaving the atom in an excited state with a hole in the core level. Resonant processes can occur only if the lifetime of the core hole ($\approx 10^{-15}$ s) is shorter than that of the excited state, which depends on the degree of localization of the electron excited in the CB. If the excited electron delocalizes faster than the core-hole lifetime, the core-hole decays through a nonresonant process with no signal enhancement in the VB spectrum. This occurrence is commonly found in metallic systems [29](see the Supplemental Material [14]). The data shown in Fig. 4 thus indicate that, relative to the time scales of the respective core-hole lifetimes ($\approx 10^{-15}$ s), the unoccupied Cr states are localized, while the N-derived states are delocalized. The intrinsic localized nature of transition metal $3d$ orbitals is very likely the origin of the experimentally observed localization of the unoccupied Cr $3d$ states, compared to the nonlocalized character of the unoccupied N $2p$ states near the CB minimum. Interestingly, because the Cr $2p$ and N $1s$ core hole lifetimes are quite similar, as indicated by the magnitude of the linewidths of the core levels, the different character of the N and Cr unoccupied states leads one to speculate that the empty Cr and N levels do not represent a single antibonding Cr-N orbital and that perhaps the empty N orbitals originate from antibonding N-O or N-N orbitals [30]. This elemental sensitive determination of the lifetime of the excited states is extremely valuable in light of the physics of photoreactivity, because it is intrinsically related to the efficiency of light-to-current conversion. When valence electrons are excited into delocalized CB states, the light-to-current conversion becomes more efficient as compared to localized states, which favor excitonic recombination (see the Supplemental Material [14]).

In summary, noncompensated codoping of rutile TiO_2 is an effective scheme for enhancing substitutional N

incorporation and for reducing the band gap toward the visible spectrum. We elucidated the precise location and nature of the impurity bands responsible for the ~1 eV band gap reduction and revealed the existence of delocalized N-derived $2p$ states near the CB minimum. The latter may be the most promising result in the context of the needed carrier mobility for photovoltaic and photocatalytic applications. Detailed spectroscopic investigations of this type are very powerful in resolving the orbital nature of impurity bands and corresponding delocalization time scales. They furthermore establish an important benchmark for testing the validity of electronic structure calculations of dopants in correlated electron materials, and for elucidating the microscopic underpinnings of dopant incorporation and activation in oxide semiconductors.

We thank Professor Z. Y. Zhang and Professor W. G. Zhu for stimulating discussions. This research was partially supported by the U.S. Department of Energy, Basic Energy Sciences, Materials Sciences and Engineering Division (H. H. W., G. E., and M. R.), and the National Science Foundation Grant No. DMR-1151687 (N. M.).

*hanno@utk.edu
†nmannell@utk.edu

[1] S. M. Sze, *Physics of Semiconductor Devices* (Wiley, New York, 1981), 2nd ed.
[2] M. Batzill and U. Diebolt, Prog. Surf. Sci. **79**, 47 (2005).
[3] X. J. Feng, K. Shankar, O. K. Varghese, M. Paulose, T. J. Latempa, and C. A. Grimes, Nano Lett. **8**, 3781 (2008).
[4] A. Fujishima and K. Honda, Nature (London) **238**, 37 (1972); Y. W. Heo, D. P. Norton, L. C. Tien, Y. Kwon, B. S. Kang, F. Ren, S. J. Pearton, and J. R. LaRoche, Mater. Sci. Rep. **47** 1 (2004); A. Kubacka, M. Fernandez-Garcia, and G. Colon, Chem. Rev. **112**, 1555 (2012); X. Chen and S. S. Mao, Chem. Rev. **107**, 2891 (2007).
[5] S. J. Pearton, W. H. Heo, M. Ivill, D. P. Norton, and T. Steiner, Semicond. Sci. Technol. **19**, R59 (2004).
[6] C. G. van de Walle and A. Janotti, Phys. Status Solidi B **248**, 1 (2011).
[7] A. Janotti, E. Snow, and C. G. Van de Walle, Appl. Phys. Lett. **95**, 172109 (2009).
[8] A. Zunger, Appl. Phys. Lett. **83**, 57 (2003).
[9] J. Robertson and S. J. Clark, Phys. Rev. B **83**, 075205 (2011).
[10] K. Obata and H. Irie, and K. Hashimoto, Chem. Phys. **339**, 124 (2007).
[11] For recent reviews, see Special issue Doping and Functionalization of Photoactive Semiconducting Metal Oxides, edited by C. Di Valentin, U. Diebold , and A. Selloni [Chem. Phys. **339**, 1 (2008)]; U. Diebold, Nat. Chem. **3**, 271 (2011).
[12] W. Zhu, X. Qiu, V. Iancu, X.-Q. Chen, H. Pan, W. Wang, N. M. Dimitrijevic, T. Rajh, H. M. Meyer, M. P. Paranthaman, G. M. Stocks, H. H. Weitering, B. Gu, G. Eres, and Z. Y. Zhang, Phys. Rev. Lett. **103**, 226401 (2009).
[13] Note that the Cr:N ratio in the present experiment is 2:1 and is different from the 1:1 ratio assumed in the DFT calculation of Ref. [12].
[14] See Supplemental Material at http://link.aps.org/supplemental/10.1103/PhysRevLett.112.036404 for details regarding sample synthesis, characterization, and spectroscopic methods.
[15] Y. Matsumoto, M. Murakami, T. Hasegawa, T. Fukumura, M. Kawasaki, P. Ahmet, K. Nakajima, T. Chikyow, and H. Koinuma, Appl. Surf. Sci. **189**, 344 (2002).
[16] As shown in Fig. 2, the Fermi level is degenerate with the CB minimum.
[17] M. Batzill, E. H. Morales, and U. Diebold, Phys. Rev. Lett. **96**, 026103 (2006).
[18] S. A. Chambers and T. Droubay, Phys. Rev. B **64**, 075410 (2001); E. S. Ilton, W. A. de Jong and P. S. Bagus, Phys. Rev. B **68**, 125106 (2003); the presence of $\mathbf{Cr}^{3+}$ is also indicated by the line shape of the Cr $\boldsymbol{L}$ edge XAS spectrum, which is very similar to the one in $\mathbf{Cr_2O_3}$ as shown by L. Soriano, M. Abbate, F. M. F. de Groot, D. Alders, J. C. Fuggle, S. Hofmann, H. Petersen, and W. Braun, Surf. Interface Anal. **20**, 21 (1993).
[19] Previous work on TiO_2 clusters has shown that the splitting is related to Cr substitutional doping; see M. Chiodi, C. Parks Cheney, P. Vilmercati, E. Cavaliere, N. Mannella, H. H. Weitering, and L. Gavioli, J. Phys. Chem. C **116**, 311 (2012).
[20] T. C. Kaspar, S. M. Heald, C. M. Wang, J. D. Bryan, T. Droubay, V. Shutthanandan, S. Thevuthasan, D. E. McCready, A. J. Kellock, D. R. Gamelin, and S. A. Chambers, Phys. Rev. Lett. **95**, 217203 (2005).
[21] F. Da Pieve, S. Di Matteo, T. Rangel, M. Giantomassi, D. Lamoen, G.-M. Rignanese, and X. Gonze, Phys. Rev. Lett. **110**, 136402 (2013).
[22] Y. Tezuka, S. Shin, A. Agui, M. Fujisawa, T. Ishii, and A. Yagishita, J. Electron Spectrosc. Relat. Phenom. **79**, 195 (1996).
[23] G. van der Laan, Phys. Rev. B **41**, 12 366 (1990).
[24] L. Soriano, M. Abbate, J. C. Fuggle, P. Prieto, C. Jimenez, J. M. Sanz, L. Galan, and S. Hofmann, J. Vac. Sci. Technol. A **11**, 47 (1993); F. Esaka, K. Furuya, H. Shimada, M. Imamura, N. Matsubayashi, H. Sato, A. Nishijima, A. Kawana, H. Ichimura, and T. Kikuchi, J. Vac. Sci. Technol. A **15**, 2521 (1997); Esaka, H. Shimada, M. Imamura, N. Matsubayashi, T. Sato, A. Nishijima, A. Kawana, H. Ichimura, T. Kikuchi, and K. Furuya, Thin Solid Films **281-282**, 314 (1996).
[25] F. Bondino *et al.*, Phys. Rev. B **82**, 014529 (2010), and references therein.
[26] P. A. Brühwiler, O. Karis, and N. Mårtensson, Rev. Mod. Phys. **74**,703 (2002).
[27] D. Menzel, Chem. Soc. Rev. **37**, 2212 (2008).
[28] P. Vilmercati, P. D. Cvetko, A. Cossaro, and A. Morgante, Surf. Sci. **603**, 1542 (2009).
[29] M. Weinelt, A. Nilsson, M. Magnuson, T. Wiell, N. Wassdahl, O. Karis, A. Föhlisch, N. Mårtnesson, J. Stöhr, and M. Samant, Phys. Rev. Lett. **78**, 967 (1997); S. Hüfner, S.-H. Yang, B. S. Mun, C. S. Fadley, J. Schäfer, E. Rotenberg, and S. D. Kevan, Phys. Rev. B **61**, 12 582 (2000).
[30] W.-J. Yin, S.-H. Wei, M. M. Al-Jassim, and Y. Yan, Phys. Rev. Lett. **106**, 066801 (2011).